INSTITUTE OF PHYSICS PUBLISHING NANOTECHNOLOGY
Nanotechnology **15** (2004) 546–550 PII: S0957-4484(04)70267-6

Large-scale synthesis of single-walled carbon nanohorns by submerged arc

H Wang[1], M Chhowalla[2], N Sano[3], S Jia[4] and G A J Amaratunga[1]

[1] University of Cambridge, Engineering Department, Trumpington Street, Cambridge CB2 1PZ, UK
[2] Rutgers University, Ceramic and Materials Engineering, Piscataway, NJ 08904, USA
[3] Himeji Institute of Technology, Department of Chemical Engineering, 2167 Shosha, Himeji 671-2201, Japan
[4] Xi'an Jiatong University, Department of Electrical Engineering, Xi'an 710049, People's Republic of China

E-mail: manish1@rci.rutgers.edu

Received 6 October 2003
Published 17 February 2004
Online at stacks.iop.org/Nano/15/546 (DOI: 10.1088/0957-4484/15/5/024)

Abstract
We report on the synthesis of single-walled carbon nanohorns (SWNHs) by arc discharge between two graphite electrodes submerged in liquid nitrogen. The product in its powder form was found to consist of spherical aggregates with sizes in the range of 50–100 nm. The nanohorns are characterized by transmission electron microscopy (TEM), Raman and electron energy loss spectroscopies and surface area measurements. TEM observations revealed that the internal structure of the aggregates could be described as a mixture of 'dahlia-like' and 'bud-like'. A structural transition above 300 °C was inferred from the Raman data. Here we show that a simple technique that does not require relatively expensive laser and vacuum equipment provides an economical alternative for the synthesis of SWNHs.

1. Introduction

Along with carbon nanotubes and fullerenes, a new form of carbon, the single walled nanohorns (SWNHs) have been synthesized. Although they were first reported by Harris *et al* [1], Iijima *et al* [2–11] showed it was possible to produce them in sizable quantities (up to 50 g h^{-1}) using laser ablation of graphite in Ar or He. The primary advantage of SWNHs is that no catalyst is required for synthesis so high purity materials can be produced. Their high surface area and excellent electronic properties have led to promising results for their use as electrode material for energy storage [9]. In addition, Iijima's group has also found remarkable methane absorption capacity, making them interesting candidates for hydrogen storage studies [10, 11]. They are projected to be technologically significant in electrodes for electrochemical cells because their unique internal structure not only contributes to a large surface area but also allows gas and liquid to permeate inside the aggregate. These novel characteristics are ideal for catalyst support and electrodes for fuel cells. Indeed, subsequent to Iijima's report [2], NEC Corporation, Japan Science and Technology Corporation and the Institute of Research and Innovation announced the fabrication of a fuel cell for mobile devices using carbon SWNHs that outperformed those fabricated from single walled carbon nanotubes (SWNTs) by an order of magnitude in terms of the energy capacity [9]. Although the potential applications are numerous, large-scale synthesis and purification of SWNTs remain critical drawbacks [12–14]. In contrast, the absence of metal catalyst allows for low cost fabrication of large quantities of high purity SWNHs.

The widely used methods to fabricate carbon nanomaterials require vacuum systems to generate plasmas using an arc discharge [15–17], laser ablation [18–20] or chemical vapour deposition [21–24]. These methods suffer in bulk production from not only the high investment and running costs of the vacuum equipment but also from low yield of the desired products. The vacuum processes also yield, in addition to the desired nanomaterials, unwanted contaminants (amorphous carbon and disordered nanoparticles) so that time consuming and costly purification steps must be carried out. Therefore, a process allowing for the generation of nanomaterials such as SWNHs with minimum contamination is desirable. Ishigami *et al* [25] proposed a high yield method for multi-walled carbon nanotubes (MWNTs) that does not require vacuum systems. In their method, an arc discharge was generated in liquid nitrogen between two carbon electrodes. After their report, an

even more economical technique using water instead of liquid nitrogen was used to successfully produce encapsulated nanotubes [26]. Working independently on the submerged arc process, we have obtained large quantities of high purity nano-onions [27–31] and SWNHs decorated with Ni nanoparticles [32]. Since then there have been several other reports on synthesis of carbon nanomaterials using the submerged arc [33, 34]. However, thus far there are no detailed reports on the large scale synthesis of SWNHs using the submerged arc.

2. Experimental details

Our submerged arc method requires only a direct current (dc) power supply, carbon electrodes and liquid nitrogen. This method is outstandingly simple and economical compared to conventional techniques used to generate carbon nanostructures such as fullerenes and nanotubes. The ability to produce significant quantities of SWNHs in a cost effective manner is an important factor for their use in energy storage applications where large quantities (kilograms) of the material are needed.

The submerged arc method used to synthesize SWNHs is identical to that used to generate carbon nano-onions in large quantities except for the fact that the liquid used is liquid nitrogen instead of de-ionized water. Briefly, a dc arc discharge was generated between two graphite electrodes submerged in 2000 cm^3 of liquid nitrogen in a stainless steel Dewar. The arc discharge was initiated in the liquid nitrogen by touching a 99.99% purity graphite anode (3 mm in diameter) with a graphite cathode (12 mm tip diameter) of similar purity. The arc voltage and current were typically 34 V and 50 A, respectively, but were also varied in some experiments in order to study their influence on the production rate. The gap between the electrodes was kept constant at around 1 mm by continuously translating the anode during the experiment in order to maintain a stable discharge. The arc discharge in liquid nitrogen is turbulent, and dense black smoke is observed near the discharge region. The evaporation rate of liquid nitrogen was about $\sim$200 cm^3 min^{-1} and the anode consumption rate was about 375.3 mg min^{-1}. In contrast to the discharge in water, the products from the arc discharge in liquid nitrogen settle exclusively at the bottom of the insulated Dewar. The products consist of MWNTs, amorphous carbon and SWNH aggregates.

3. Results and discussion

The settled powders from the bottom of the Dewar were collected by adding de-ionized water to the Dewar and pouring the products into a clean 500 ml beaker. Surprisingly, it was found that a natural segregation of the powder constituents takes place. In de-ionized water, the powder separates into three phases, one remaining floating at the water surface, one floating in suspension and one settling at the bottom. The floating products were collected by skimming a glass slide along the water surface. The glass slide was then rinsed with de-ionized water. The products in suspension were collected using a pipette. The collected products were then allowed to dry at room temperature for several days. The production rate was measured by drying the powder on a hot plate to remove any excess water and measuring the weight. The highest production rate of the floating and suspended powders was found to be 17 g h^{-1} when a 3 mm anode and 100 A current were used, respectively. We have found that the powder floating at the surface and that remaining in suspension were similar, consisting of aggregates containing 'dahlia-like' and 'bud-like' SWNHs [2–11]. A scanning electron microscopy (SEM) image of the floating powder produced in liquid nitrogen is shown in figure 1(a). The powder was found to consist of uniform spherical aggregates ranging in size from 50–100 nm with detailed SEM examination revealing practically no polyhedral graphitic fragments or elongated nanotube particles. Closer examination of the aggregates using a TEM revealed two types of structures as shown in figure 1(b). The samples for TEM were prepared by sprinkling the dried powder onto a holey carbon grid. The larger image in figure 1(b) shows a low magnification image of the structures present in the powder. Expanded regions from this image shown in figures 1(c)–(e) reveal the internal structure of the aggregates. Figures 1(c) and (e) show the 'dahlia-like' structure while figure 1(d) shows the 'bud-like' internal structure of the aggregates. We estimate from our TEM analysis that our powder contains approximately 55% 'dahlia-like' aggregates, and 45% 'bud-like' aggregates. A higher resolution image of SWNHs protruding from the 'dahlia-like' aggregate is shown in figure 1(e). Single walled structures protruding from a core can be clearly observed. The measured open angle of the tip of the structures was found to be in the range of 20°–30°, in agreement with results of Iijima *et al* [2]. Furthermore, selected area electron diffraction does not show

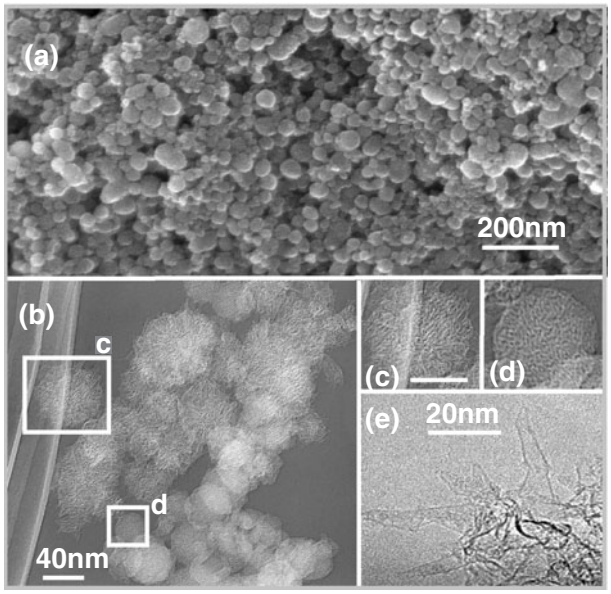

Figure 1. Scanning electron microscope image of circular nanohorn aggregates ranging from 50–100 nm in diameter. The powder that remained in suspension also showed similar structures. The SEM was performed on a JEOL 6340 FEGSEM operated at 5 kV and a working distance of 3 mm. The samples for TEM were prepared by sprinkling the dried powder onto a holey carbon grid. The TEM was performed using a JEOL 2010FX microscope operated at 200 kV. (b) Low magnification TEM image of nanohorns. (c) Enlargement of aggregates with 'dahlia-like' internal structure. (d) Enlargement of an aggregate with 'bud-like' aggregates. (e) High-resolution TEM image of 'dahlia-like' aggregates showing single walled nanohorns.

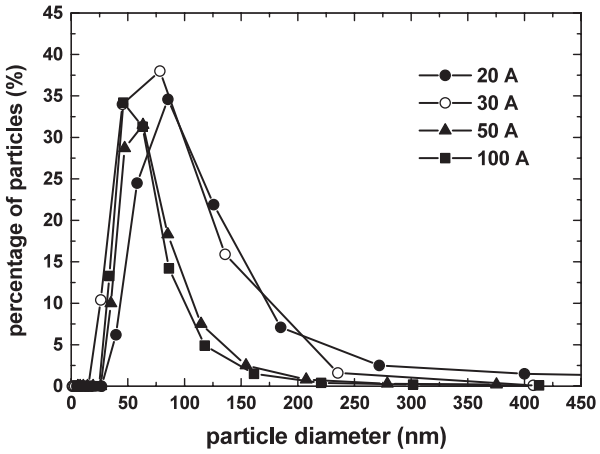

Figure 2. Direct light scattering (DLS) measurements on SWNH powder dispersed in toluene. The particle size distributions shown are from four samples produced at varying arc currents.

any (0001) spacing, indicating that the aggregates shown in figure 1 consist of single walled structures, as confirmed by the high-resolution image in figure 1(e).

A more detailed particle size distribution analysis of the as-produced powder was performed using dynamic laser scattering (DLS). The DLS samples were prepared by ultrasonication in 30 s intervals for 30 min in toluene. The measurement was carried out by using a 633 nm laser with a controlled temperature of 20 °C. The DLS measurements of the SWNHs aggregates as a function of different arc currents is shown in figure 2. The results indicate that the average particle size of the SWNHs aggregates decreases with arc current. Furthermore, the particle size distribution is also narrower at higher arc currents. The mean particle size sharply decreased from ∼110 to ∼70 nm when the arc current was increased from 20 to 50 A, and gradually decreased to 60 nm at an arc current of 100 A. The DLS measurements agree well with our SEM analysis of the aggregate size distribution.

In order to understand the structural properties and formation mechanism of our SWNHs in greater detail, we performed electron energy loss (EELS) and Raman spectroscopies. The EELS and Raman studies were performed as a function of temperature in order to monitor any structural changes and nitrogen evolution. The as-produced SWNH aggregates were annealed in a furnace with flowing Ar at five different temperatures. The EELS analysis was performed with a parallel detector fitted to a Topcon 200 kV TEM. The EEL spectra as a function of temperature are shown in figure 3. All spectra show the carbon K-edge with π^* and σ^* peaks at 285 and 289 eV, respectively, indicative of sp^2 graphite-like bonding. A closer examination of the carbon K-edge features reveals that the features become sharper with temperature, indicating ordering of the sp^2 phase. Indeed, the EELS edges of samples annealed above 300 °C indicated a greater degree of ordering than those annealed at lower temperature. The variation of the π^* peak towards more ordered graphite structure indicates a phase change during annealing. The carbon K-edge at 500 °C is comparable to highly oriented pyrolytic graphite (HOPG). In addition to the carbon K-edge, the nitrogen K-edge with π^* and σ^* peaks at 398 and 400 eV, respectively, is also visible in samples

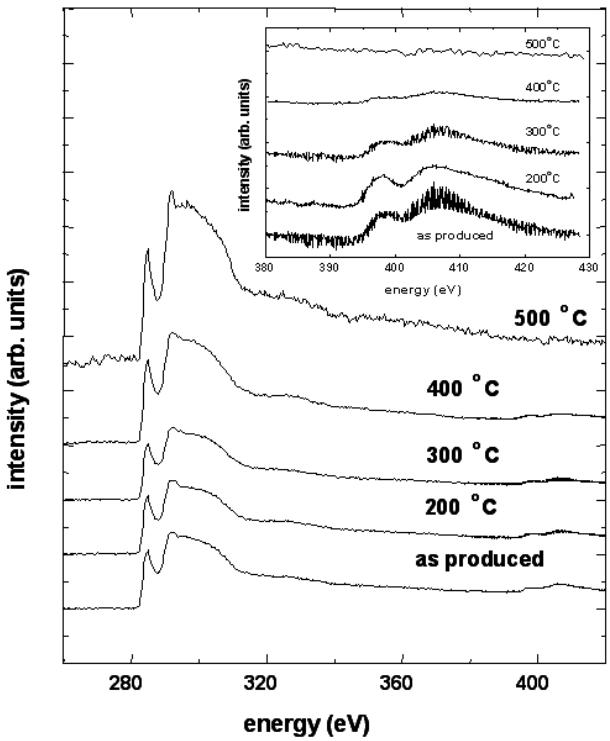

Figure 3. Electron energy loss spectra (EELS) of SWNH powders annealed at four different temperatures. The inset shows the nitrogen K-edge in greater detail for clarity. Note that at an annealing temperature of 500 °C, no nitrogen is detected by EELS.

annealed below 400 °C, as shown in the inset of figure 3. The nitrogen content is found to decrease gradually with the annealing temperature, and no nitrogen is detected when the powder is annealed above 500 °C. The EELS data indicate that nitrogen incorporation during SWNH formation occurs. However, it is unclear how the nitrogen is incorporated. That is, it is unclear if nitrogen is trapped in gaseous form, whether it is incorporated into the graphene sheet forming the SWNHs, or if it forms a volatile amorphous CN_x compound during the discharge. The fact that the nitrogen concentration gradually decreases as a function of annealing temperature indicates that trapped nitrogen is being released. If bonded nitrogen was present as either volatile CN_x or within the graphene sheet, then evolution of nitrogen should occur sharply at a specific temperature. Instead a gradual decrease in nitrogen content is observed, indicating the presence of trapped gaseous nitrogen. The nitrogen release mechanism may be related to the formation of holes in the nanohorn wall during annealing. Our surface area measurements indicate that an opening in the horn wall can be introduced through annealing in air (see below). As the nanohorns powder is heated, remnant air in our annealing furnace may induce holes in the nanohorns wall through oxidation, allowing the trapped nitrogen to escape.

The Raman spectroscopy results as a function of the annealing temperature are shown in figure 4. The Raman analysis was performed with a Renishaw spectrometer with a 514.5 nm Ar ion laser. A structural transition in our SWNHs can be inferred from our Raman data. The Raman spectrum of as-produced SWNHs show typical nanocarbon disorder D (at ∼1350 cm^{-1}) and G (∼1580 cm^{-1}) peaks. No dramatic

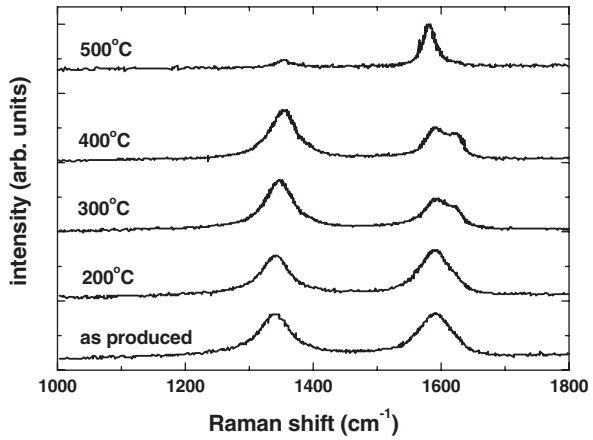

Figure 4. Raman spectra of SWNH powders annealed at four different temperatures. A transition towards graphite is inferred through the change in shape of the G peak. The suppression of the D peak and the rise of a sharp G peak at 500 °C is indicative of graphitization.

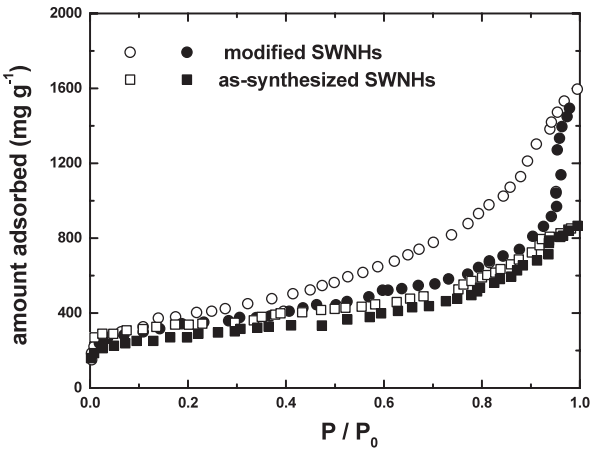

Figure 5. Nitrogen adsorption isotherms taken at 77 K for as-produced and modified SWNHs (oxidized in air at 350 °C).

change in the Raman features is observed upon annealing up to 200 °C. However, above 200 °C the relative intensity of the D peak increases in comparison to the G peak. Furthermore, the structure of the G peak also changes dramatically at annealing temperatures of 300 and 400 °C. G peak splitting is also clearly visible. The spectra for samples annealed above 200 °C are similar to those for glassy carbon. The changes in the G peak shape and the intensity ratios of the D and G peak indicate that a structural transition from nanocarbon to amorphous/glassy state has taken place. These results are comparable to those reported by Kasuya *et al* [5]. Finally, the Raman analysis indicates that further annealing leads to almost complete graphitization of our nanohorns at 500 °C. At 500 °C, the D peak is almost completely suppressed while a single sharp G peak is present.

The specific surface area of the as-produced SWNH powder was determined by nitrogen gas adsorption based on a Brunauer–Emmett–Teller (BET) adsorption isotherm using an automated surface area analyser (Coulter, OMNISORP100). The samples were annealed for several hours at 150 °C in a vacuum (10^{-4} Pa) furnace prior to initiating the surface area measurements. The results reveal values of ∼1000–1500 $m^2\ g^{-1}$ significantly larger than those reported for single and multi-walled carbon nanotubes (SWNT and MWNT) [35]. The nitrogen adsorption isotherms carried out at 77 K are shown in figure 5 for samples with two different surface areas. It can be seen that the higher surface area sample (modified) adsorbs more nitrogen than the one with a lower surface area. The larger surface area was induced by oxidizing the SWNHs by heating in air at 200 °C for several hours. Furthermore, oxidation leads to the enhancement of nitrogen adsorption and also leads to an adsorption hysteresis. The hysteresis is attributed to the creation of mesopores [10, 11] in the SWNH aggregates. We believe that this is due to the incorporation of openings in individual nanohorns that enhance the surface area and create reactive adsorption sites. These results are also comparable to those reported by Iijima *et al* [2–11] indicating that our SWNHs are comparable.

The production rate of our SWNHs is 17 g h^{-1}. Although this is less than Iijima's process (50 g h^{-1}) [5], our process is simpler and significantly less expensive. It should also be noted that our process has not yet been optimized. The formation mechanism of nanohorn aggregates is complicated and is probably similar to that in laser ablation [5]. The high pressure and temperature make it difficult to determine the exact conditions within the growth zone. The conditions used here are comparable to those outlined by Kasuya *et al* [5]. In their case [5], they find mostly 'bud-like' nanohorns when argon is replaced by nitrogen during laser ablation of graphite. Our results are similar since we see almost a mixture of 'dahlia-like' and 'bud-like' nanohorns. The arc discharge in liquid nitrogen is similar to laser ablation in 760 Torr of nitrogen in that the very high local temperatures of the arc spot (up to 4400 K) vaporize the surrounding liquid, creating a bubble of nitrogen gas. The graphite evaporation due to the arc occurs essentially in atmospheric pressure of nitrogen. Furthermore, the plasma emitted by arc evaporation has comparable properties to laser ablation plasma. Therefore, we can create conditions similar to the laser ablation system but without the costly vacuum equipment. The conditions created in our submerged arc apparatus appear to be favourable for the formation of SWNHs. Specifically, the high density of nitrogen creates rapid quenching of carbon species and low diffusion rate, allowing the formation of graphene sheets. Simulations by Kawai *et al* [36] have shown that aggregates consisting of nanohorns could be formed from the graphene sheets. Iijima *et al* [2] have argued that the uniform diameter of the 'dahlia-like' SWNHs may indicate that formation occurs via rapid quenching from a liquid state.

4. Conclusions

In conclusion, we report on a simple technique for the fabrication of SWNHs. SEM and TEM investigations reveal the presence of circular aggregates. The internal structures of the aggregates correlated to 'dahlia-like' and 'bud-like' nanohorns. The ability to fabricate relatively large quantities (17 g h^{-1}) of nanohorns without optimizing our apparatus provides an alternative synthesis route for these technologically significant materials. The SWNHs produced using this method were found to be structurally similar to those produced by Iijima *et al* [2]. The surface area measurements indicate that these materials could be useful for gas adsorption.

References

[1] Harris P J F, Tsang S C, Claridge J B and Green M L H 1994 High resolution electron microscopy studied of a microporous carbon produced by arc evaporation *J. Chem. Soc. Faraday. Trans.* **90** 2799–802

[2] Iijima S, Yudasaka M, Yamada R, Bandow S, Suenaga K, Kokai F and Takahashi K 1999 Nano-aggregates of single-walled graphitic carbon nanohorns *Chem. Phys. Lett.* **309** 165–70

[3] Takikawa T, Ikeda M, Hirahara K, Hibi Y, Tao Y, Ruiz P A, Sakakibara T, Itoh S and Iijima S 2002 Fabrication of single-walled carbon nanotubes and nanohorns by means of a torch arc in open air *Physica* B **323** 277–9

[4] Bandow S, Kokai F, Takahashi K, Yudasaka M, Qin L C and Iijima S 2000 Interlayer spacing anomaly of single-wall carbon nanohorn aggregate *Chem. Phys. Lett.* **321** 514–9

[5] Kasuya D, Yudasaka M, Takahashi K, Kokai F and Iijima S 2002 Selective production of single-wall carbon nanohorn aggregates and their formation mechanism *J. Phys. Chem.* B **106** 4947–51

[6] Murata K, Kaneko K, Steele W A, Kokai F, Takahashi K, Kasuya D, Yudasaka M and Iijima S 2001 Porosity evaluation of intrinsic intraparticle nanopores of single wall carbon nanohorn *Nano Lett.* **1** 197–9

[7] Murata K, Kaneko K, Kokai F, Takahashi K, Yudasaka M and Iijima S 2000 Pore structure of single-wall carbon nanohorn aggregates *Chem. Phys. Lett.* **331** 14–20

[8] Kokai F, Takahashi K, Kasuya D, Yudasaka M and Iijima S 2002 Growth dynamics of single-wall carbon nanotubes and nanohorn aggregates by CO_2 laser vaporization at room temperature *Appl. Surf. Sci.* **197** 650–5

[9] 2001 NEC news: NEC uses carbon nanotubes to develop a tiny fuel cell for mobile applications—a big step for next-generation energy with nanotechnology NEC electronics (Europe) at http://www.ee.nec.de/News/Releases/pr283-01.html (August, 2001)

[10] Bekyarova E, Murata K, Yudasaka M, Kasuya D, Iijima S, Tanaka H, Kahoh H and Kaneko K 2003 Single-wall nanostructured carbon for methane storage *J. Phys. Chem.* B **107** 4681–4

[11] Bekyarova E, Kaneko K, Kasuya D, Takahashi K, Kokai F, Yudasaka M and Iijima S 2001 Pore structures and methane adsorptivity of SWNHs treated in different atmospheres *ISNC: Proc. Int. Symp. Nanocarbons (Nagano, Japan, Nov. 2001)* pp 141–2

[12] Zhou W, Ooi Y H, Russo R, Papanek P, Luzzi D E, Fischer J E, Bronikowski M J, Willis P A and Smalley R E 2001 Structural characterization and diameter-dependent oxidative stability of single wall carbon nanotubes synthesized by the catalytic decomposition of CO *Chem. Phys. Lett.* **350** 6–14

[13] Rinzler A G, Liu J, Dai H, Nikolaev P, Huffman C B, Rodriguez-Macias F J, Boul P J, Lu A H, Heymann D, Colbert D T, Lee R S, Fischer J E, Rao A M, Eklund P C and Smalley R E 1998 Large-scale purification of single-wall carbon nanotubes: process, product, and characterization *Appl. Phys.* A **67** 29–37

[14] Liu J, Rinzler A G, Dai H J, Hafner J H, Bradley R K, Boul P J, Lu A, Iverson T, Shelimov K, Huffman C B, Rodriguez-Macias F, Shon Y S, Lee T R, Colbert D T and Smalley R E 1998 Fullerene pipes *Science* **280** 1253–6

[15] Ebbesen T W and Ajayan P M 1992 Large scale synthesis of carbon nanotubes *Nature* **358** 220–2

[16] Journet C, Maser W K, Bernier P, Loiseau A, de la Chapelle M L, Lefrant S, Deniard P, Lee R and Fischer J E 1997 Large-scale production of single-walled carbon nanotubes by the electric-arc technique *Nature* **388** 756–8

[17] Ando Y, Zhao X L, Inoue S and Iijima S 2002 Mass production of multiwalled carbon nanotubes by hydrogen arc discharge *J. Cryst. Growth* **237** 1926–30

[18] Scott C D, Arepalli S, Nikolaev P and Smalley R E 2001 Growth mechanisms for single-wall carbon nanotubes in a laser-ablation process *Appl. Phys.* A **72** 573–80

[19] Geohegan D B, Schittenhelm H, Fan X, Pennycook S J, Puretzky A A, Guillorn M A, Blom D A and Joy D C 2001 Condensed phase growth of single-wall carbon nanotubes from laser annealed nanoparticulates *Appl. Phys. Lett.* **78** 3307–9

[20] Thess A, Lee R, Nikolaev P, Dai H J, Petit P, Robert J, Xu C H, Lee Y H, Kim S G, Rinzler A G, Colbert D T, Scuseria G E, Tomanek D, Fischer J E and Smalley R E 1996 Crystalline ropes of metallic carbon nanotubes *Science* **273** 483–7

[21] Zhang R Y, Amlani L, Baker J, Tresek J and Tsui R K 2003 Chemical vapor deposition of single-walled carbon nanotubes using ultrathin Ni/Al film as catalyst *Nano Lett.* **3** 731–5

[22] Cui H, Eres G, Howe J Y, Puretkzy A, Varela M, Geohegan D B and Lowndes D H 2003 Growth behavior of carbon nanotubes on multilayered metal catalyst film in chemical vapor deposition *Chem. Phys. Lett.* **374** 222–8

[23] Cumings J, Mickelson W and Zettl A 2003 Simplified synthesis of double-wall carbon nanotubes *Solid State Commun.* **126** 359–62

[24] Bronikowski M J, Willis P A, Colbert D T, Smith K A and Smalley R E 2001 Gas-phase production of carbon single-walled nanotubes from carbon monoxide via the HiPco process: a parametric study *J. Vac. Sci. Technol.* A **19** 1800–5

[25] Ishigami M, Cumings J, Zettl A and Chen S 2000 A simple method for the continuous production of carbon nanotubes *Chem. Phys. Lett.* **319** 457–9

[26] Hsin Y L, Hwang K C, Chen F R and Kai J J 2001 Production and *in situ* metal filling of carbon nanotubes in water *Adv. Mater.* **13** 830–2

[27] Sano N, Wang H, Chhowalla M, Alexandrou I and Amaratunga G A J 2001 Nanotechnology—synthesis of carbon 'onions' in water *Nature* **414** 506–7

[28] Sano N, Wang H, Alexandrou I, Chhowalla M, Teo K B K, Amaratunga G A J and Iimura K 2002 Properties of carbon onions produced by an arc discharge in water *J. Appl. Phys.* **92** 2783–8

[29] Sano N, Wang H L, Chhowalla M, Alexandrou I, Amaratunga G A J, Naito M and Kanki T 2003 Fabrication of inorganic molybdenum disulfide fullerenes by arc in water *Chem. Phys. Lett.* **368** 331–7

[30] Roy D, Chhowalla M, Wang H, Sano N, Alexandrou I, Clyne T W and Amaratunga G A J 2003 Characterisation of carbon nano-onions using Raman spectroscopy *Chem. Phys. Lett.* **373** 52–6

[31] Chhowalla M, Wang H, Sano N, Teo K B K, Lee S B and Amaratunga G A J 2003 Carbon onions: carriers of the 217.5 nm interstellar absorption feature *Phys. Rev. Lett.* **90** 155504

[32] Sano N, Kikuchi T, Wang H, Chhowalla M and Amaratunga G A J 2004 Carbon nanohorns hybridized with a metal-included nanocapsule *Carbon* **42** 95–9

[33] Lange H, Sioda M, Huczko A, Zhu Y Q, Kroto H W and Walton D R M 2003 Nanocarbon production by arc discharge in water *Carbon* **41** 1617–23

[34] Antisari M V, Marazzi R and Krsmanovic R 2003 Synthesis of multi walled nanotubes by electric arc discharge in liquid environments *Carbon* **41** 2393–401

[35] Inoue S, Ichikuni N, Suzuki T, Uematsu T and Kaneko K 1998 Capillary condensation of N_2 on multiwall carbon nanotubes *J. Phys. Chem.* B **102** 4689–92

[36] Kawai T, Miyamoto Y, Sugino O and Koga Y 2002 Nanotube and nanohorn nucleation from graphitic patches: tight-binding molecular-dynamics simulations *Phys. Rev.* B **66** 033404